PROCEEDINGS OF SCIENCE

Effect of the knock-on electrons in the calorimetric mode of an underground muon detector

M. Scornavacche,[a,b,*] **J.M. Figueira,**[a] **F. Sánchez**[a] **and D. Veberič**[b]

[a] *Instituto de Tecnologías en Detección y Astropartículas (CNEA, CONICET, UNSAM), Av. Gral. Paz 1499, Buenos Aires, Argentina*

[b] *Institut für Astroteilchenphysik (IAP), Karlsruher Institut für Technologie (KIT), Hermann-von-Helmholtz-Platz 1, 76344 Eggenstein-Leopoldshafen, Germany*

E-mail: marina.scornavacche@iteda.gob.ar

Calibrating underground detectors necessitates careful consideration of the passage of penetrating particles through matter. In muon detectors based on plastic scintillators, like the Underground Muon Detector of the Pierre Auger Observatory, the energy deposition within the plastic is significantly influenced by the generation of delta (knock-on) electrons in the surrounding ground as muons pass through. In this study, we analyzed the energy deposition by various particles impacting a 2.3 m deep underground detector and assessed its effect on the reconstruction of muon density in extensive air showers induced by energetic nuclei. Our results reveal that calibrating the calorimetric mode of these detectors using individual vertical muons introduces a reconstruction bias of up to 20% for proton showers with energies of $10^{17.5}$ eV. This bias arises from an increased energy deposition per muon, particularly near the shower axis, where more energetic muons are generated and, therefore, more knock-on electrons are produced.

7th International Symposium on Ultra High Energy Cosmic Rays (UHECR2024)
17-21 November 2024
Malargüe, Mendoza, Argentina

*Speaker

ISSN 1824-8039. Published by SISSA Medialab.

PoS(UHECR2024)116

1. Introduction

To interpret the readings of underground muon scintillation detectors that are used for the study of extensive air showers, it is necessary to consider the transmission of different particles that reach the observation level through the ground and to take into account showers of secondary particles in the ground that also induce signals in underground muon detectors [1].

In an inelastic collision with atoms, an energetic charged particle transfers energy to the electrons bound in orbitals. When the energy transferred to the electron is higher than its ionization energy, the electron is ejected from its atomic orbital. The term knock-on electron is utilized for electrons that are ejected from their orbit and additionally have sufficient kinetic energy to travel a significant distance from its point of ejection [2]. Collectively, these electrons are defined as δ-rays when they have sufficient energy to produce secondary interactions and ionize further atoms in areas distant from the primary particle beam. The production of knock-on electrons by underground cosmic-ray muons has been documented in several studies, for example in Refs. [3, 4]. The higher the energy of the muon at the ground, the greater is the energy transferred to the electrons, enabling them to traverse longer distances and enhancing their chances of reaching the underground scintillators. In certain situations knock-on electrons may prevent the accurate determination of the number of muons that hit an underground detector.

An in-depth exploration of the Underground Muon Detector (UMD) of the Pierre Auger Observatory can be found in Ref. [5]. In the final design, exhibited in the left panel of Fig. 1, three modules of 10 m^2 are buried at 2.3 m next to a water-Cherenkov detector. Each module consists of 64 plastic scintillator strips containing wavelength shifting optical fiber connected to an array of 64 silicon photomultipliers (SiPMs) (see right panel of Fig. 1). When a muon impinges the scintillator, the photons produced are collected and propagated along the fibers to the photodetector. The calorimetric mode of the UMD operates by treating the module as a single unit, independent of its internal segmentation. In this mode, the signals from all 64 SiPMs are summed and then amplified through two separate channels using high- and low-gain amplifiers. The amplified signal of each channel is digitized with a sampling interval of 6.25 ns, resulting in a waveform of 1024 samples. Finally, the integrated charge from the combined signals is calculated and stored. The low-gain (LG) channel in this mode extends the dynamic range of the detector, allowing it to measure high muon densities near the shower core. It is worth noting that this acquisition mode in the UMD is commonly referred to as the *ADC* or *integrator*.

The potential influence of the energy deposited by knock-on electrons on this detection mode remains unexplored. Hence, this study aims to estimate the impact of these knock-on electrons on the muon reconstruction bias.

2. Bias in muon reconstruction

Monte-Carlo simulations of proton showers were performed (simulated with the hadronic interaction model EPOS-LHC) at energies of $10^{17.5}$, 10^{18}, and $10^{18.5}$ eV and zenith angles of 0, 12, 22, 32, and 38 degrees. The secondary particles of the shower that reached ground level were propagated through the soil and the energy deposition in the UMD was calculated using Geant4 [6].

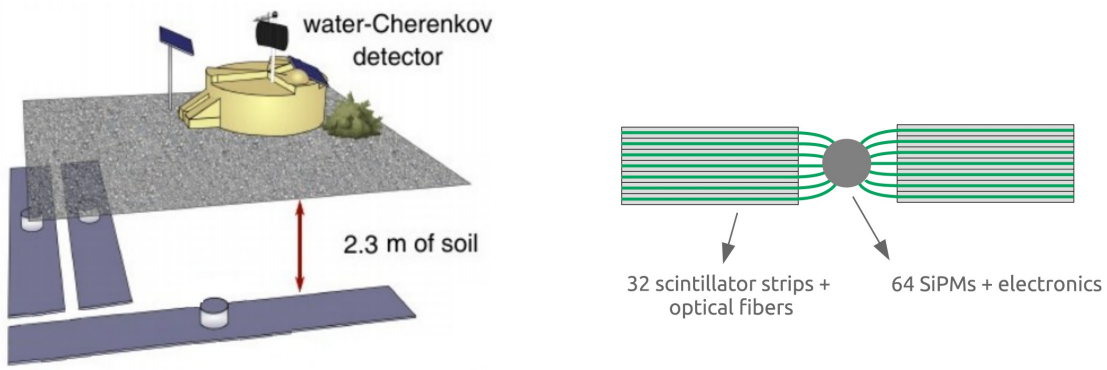

Figure 1: (left) Schematics of the final UMD design with three modules of 10 m^2. (right) Schematics of an UMD module.

The response of the detector was simulated in Offline [7], the official software of the Pierre Auger Observatory. Saturated modules were excluded from the analysis.

In the ADC mode the number of muons impinging a 10 m^2 UMD module can be estimated by

$$N_\mu^{\mathrm{ADC}} = \frac{q_{\mathrm{meas}} \cos\theta}{\langle q_{1\mu}(\theta{=}0)\rangle}, \tag{1}$$

where the quantity in the numerator is the total charge per vertical path length in the event, with q_{meas} the measured charge in a 10 m^2 UMD module. The quantity in the denominator, $\langle q_{1\mu}(\theta{=}0)\rangle$, is the mean charge deposited by individual vertical muons. The approximation $\langle\theta_\mu\rangle \approx \theta_{\mathrm{shower}}$ is employed, considering that in the field it is not feasible to measure the zenith angle of each muon impinging on the scintillator.

The bias in the reconstruction of the muon number, under the assumption that the mean charge deposited by individual vertical muons is independent of the distance to the shower axis, as proposed in Ref. [8], is shown in Fig. 2 as a function of the number of injected muons per 10 m^2 module (N_μ^{Inj}). Two horizontal dashed lines indicate the region where the absolute value of the bias is below 5%. The reconstruction bias for events with less than ~5 muons in a 10 m^2 module remains below 5%, indicating that for such low muon densities, Eq. (1) and the assumption of a constant average charge (independent of the distance to the shower axis) deposited by individual vertical muons perform reasonably well. However, the figure reveals a concerning trend: the reconstruction bias increases with muon density across all energy bins considered. This implies that the bias becomes more severe closer to the shower axis, reaching up to 20% for $10^{17.5}$ eV energy showers with muon densities of around 300 muons per 10 m^2 module. The subsequent sections aim to explore the source of this bias.

3. Zenith-angle approximation for muons

The difference between the average zenith angle of the muons injected into a 10 m^2 module ($\langle\theta_\mu\rangle$) and the zenith angle of the shower they originate from (θ_{shower}) is displayed in the left panel of Fig. 3 as a function of the number of injected muons per 10 m^2 module. In the right panel, the bias introduced by the approximation $\cos\langle\theta_\mu\rangle \approx \cos\theta_{\mathrm{shower}}$ in Eq. (1) is illustrated. Across all

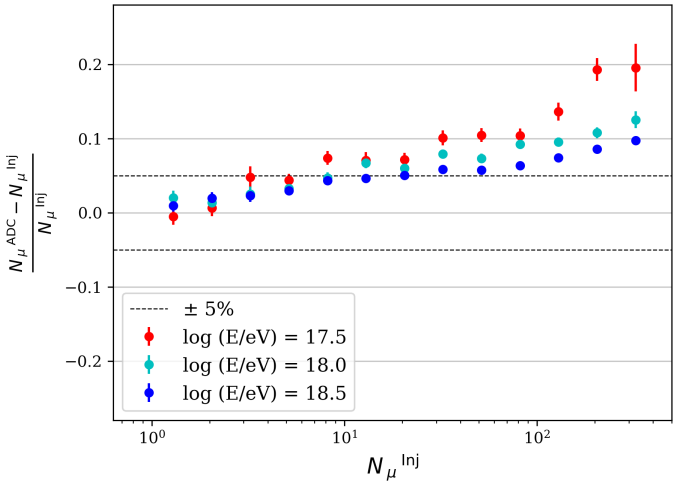

Figure 2: Bias obtained in the muon reconstruction with the ADC mode as a function of the number of injected muons per 10 m^2 module.

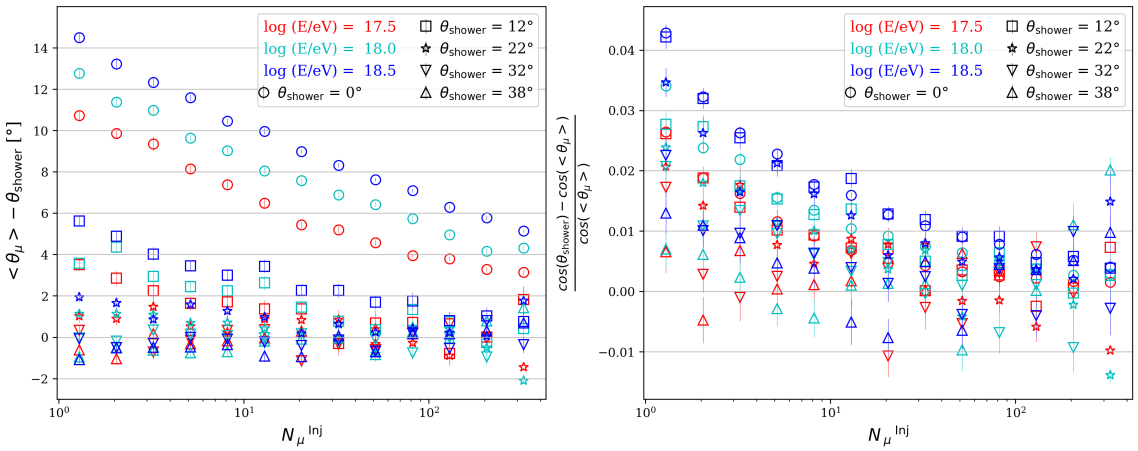

Figure 3: (Left) Difference between the average zenith angle of the muons injected into a 10 m^2 module and the zenith angle of the shower they originate from, as a function of the number of injected muons per 10 m^2 module. (Right) Bias introduced in the muon reconstruction from the approximation $\cos\langle\theta_\mu\rangle \approx \cos\theta_{\rm shower}$ as a function of the number of injected muons per 10 m^2 module.

energy bins, the absolute bias $\langle\theta_\mu\rangle - \theta_{\rm shower}$ and its effect on the relative bias in the reconstructed muon number are more significant for low muon densities, vertical showers, and the most energetic events, reaching maximum values of approximately 14 degrees and 4%, respectively. As can be seen, the absolute bias of the zenith angle decreases with the distance to the shower core, with the relative bias in the reconstructed muon number dropping to less than 2% for muon densities of about 300 muons per 10 m^2 module. Consequently, the bias observed in Fig. 2, reaching up to 20% for muon densities of about 30 μ/m^2, cannot be attributed to the approximation $\cos\langle\theta_\mu\rangle \approx \cos\theta_{\rm shower}$ in Eq. (1).

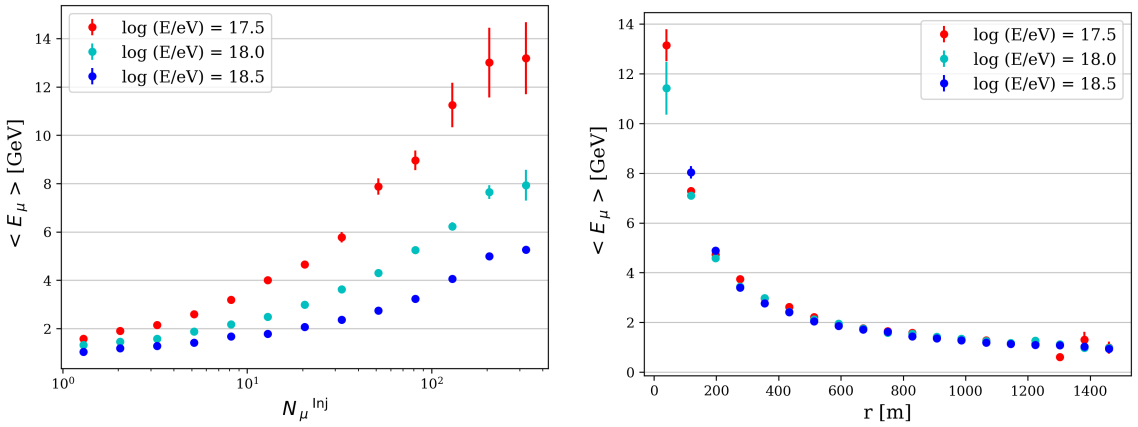

Figure 4: (left) Average energy $\langle E_\mu \rangle$ of muons arriving at the UMD as a function of the number N_μ^{Inj} of injected muons per 10 m^2 module. (right) Average energy $\langle E_\mu \rangle$ of muons arriving at the UMD as a function of the distance r to the shower core.

4. Energy deposited in the scintillators

In Fig. 4, the average energy of muons arriving to a UMD module, obtained as an average across all zenith angle bins, is depicted as a function of the number of injected muons per 10 m^2 module (left panel) and as a function of the distance to the shower core (right panel). As can be seen, more energetic muons correspond to higher muon densities, since the muon energy increases closer to the shower axis. For a fix muon density, the average energy of muons rises as the energy of the shower decreases. In the following analysis, we present how this increase in muon energy influences the energy deposited in the UMD scintillators.

The total energy deposited in the UMD scintillators per injected muon per vertical path length was calculated as

$$\frac{E^{\text{total}}_{\text{deposited}} \cos\langle\theta_\mu\rangle}{N_\mu^{\text{Inj}}}, \tag{2}$$

where the term $\cos\langle\theta_\mu\rangle$ corrects for the fact that more inclined muons traverse a longer path within the scintillator than vertical muons, leading, of course, to higher energy deposition. A histogram of the energy deposited per muon per unit vertical path length, constructed using the complete dataset with the restriction of excluding saturated modules, is shown in the left panel of Fig. 5. The average deposited energy is (2.101 ± 0.004) MeV. In the right panel of Fig. 5, the average energy deposited per muon per vertical path length is depicted as a function of the average muon energy. The energy deposited exclusively by muons is represented with blue circles, whereas the total energy deposited is displayed with orange circles. Firstly, it can be noted that when a muon arrives at the UMD with less than ~0.3 GeV, the average energy deposited per muon rises rapidly as muon energy decreases. For muon energies lower than this threshold, the behavior as a minimum ionizing particle ceases and, consequently, the muon energy-loss rate exhibits a rapid rise as expected in the low energy range of the Bethe regime [9], generating an average energy deposited of up to 10 MeV. Secondly, the average total energy deposited reaches a minimum of approximately 1.8 MeV for muon energies of around 0.3 GeV. Above this point, as the muon energy increases, the total energy deposited per

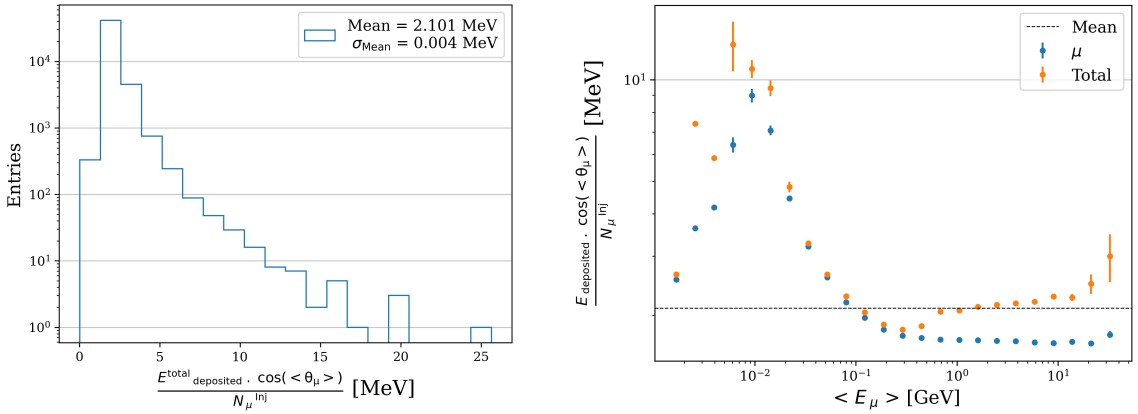

Figure 5: (left) Histogram of the total energy deposited per muon per vertical path length in the UMD scintillators. (right) Energy deposited per muon per vertical path length as a function of the average energy of muons arriving in the UMD. Two cases are displayed: the energy deposited by exclusively muons (blue) and the total energy deposited by all the particles (orange).

muon per vertical path length exhibits a rapid increase, reaching a ∼35% larger value for a muon energy of 20 GeV. However, as can be seen, the energy deposited per muon per vertical path length by exclusively muons remains nearly constant in the same energy range. Therefore, the observed rise in total energy deposition indicates the involvement of additional particles beyond muons (mainly knock-on electrons, as it will be shown below) in the contribution to the energy deposition in the scintillators.

The particles that are most likely to arrive in the UMD scintillators are $\mu^{\pm}$, γ, $e^{\pm}$, $p^{\pm}$, $\nu_{\mu}^{\pm}$ and $\nu_{e}^{\pm}$. Any other particle observed is categorized as "Other". In the performed simulations, we observed "Other" particles such as π^{+} and K^{+} (along with their corresponding antiparticles), K_{L}^{0}, K_{S}^{0} and $\bar{\Lambda}$. The number of particles increases close to the shower core, as expected. A crucial question to address is whether arriving electrons at the UMD were knock-on electrons, produced in the soil due to the passage of muons, or punch-through electrons, belonging to the electromagnetic component of the air shower. Then, we compare these results with simulations where only muons were allowed to be injected into the ground.

In Fig. 6, the fraction of the energy deposited is displayed for the different types of particles as a function of the number of injected muons per 10 m^2 module, for showers of $10^{17.5}$ eV (left panel) and $10^{18.5}$ eV (right panel). The simulations where all particles were injected into the ground and propagated through the soil are displayed with filled circles, while the simulations where only muons were injected are depicted with unfilled rectangles. This analysis was conducted including the saturated modules, with the aim of illustrating the impact of other particles beyond the scope of our muon measurements. A dashed vertical line indicates the maximum number of injected muons that the detector measured without saturating. Once this limit is reached, the detector saturates and no muon reconstruction can be performed. In our regime of muon measurements, several conclusion can be drawn. Firstly, upon comparing both sets of simulations, we observe that the energy-deposit fractions for muons (blue), electrons (violet), and photons (orange) are quite similar, therefore punch-through electrons and photons reaching the UMD are negligible and electrons and

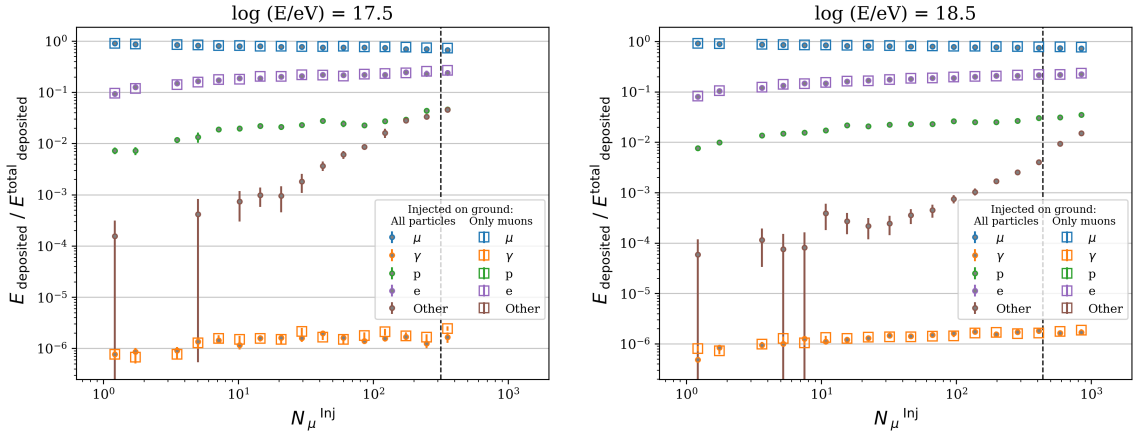

Figure 6: Fraction of energy deposited by the different types of particles as a function of the number of injected muons per 10 m^2 module, for the two sets of simulations: all particles injected into the ground (filled circles) and only muons (unfilled rectangles). A dashed line denotes a rough estimate of the saturation.

photons depositing energy into the UMD originated from the passage of muons through the soil. It is worth noting that, as expected, no protons or particles categorized as "Other" (e.g., π^+ and K^+) were found when only muons were injected and, consequently, these are punch-through particles arriving at the UMD which do not belong to the muon component of the shower. Secondly, upon analyzing the energy deposited when all particles were injected (filled circles), we can deduce that the main contributions primarily come from muons and electrons, where electrons can contribute up to around 23% of the total energy deposited near the shower axis. Photons have a negligible contribution to the total energy deposit. Excluding muons, the primary contribution comes from knock-on electrons, but protons and other particles also play a role, especially near the shower core where their contribution can reach up to 8% for $10^{17.5}$ eV showers. This contribution becomes less significant for higher energy showers within the range of our muon measurements.

In Fig. 7, we present the fraction of energy deposited by particles other than muons. In the left panel, this fraction is exhibited as a function of the number N_μ^{Inj} of injected muons per 10 m^2 module. We observe that the fraction of energy deposited by other particles rises with the muon densities, reaching up to 31% of the total energy for low energy showers. This effect is more pronounced for less energetic showers, since at the same muon density they tend to have more energetic muons (see Fig. 4). For each bin of N_μ^{Inj}, we calculated the bias in the muon reconstruction as a function of the fraction of energy deposited by particles excluding muons. In the right panel, we show that the bias increases in accordance with the increase in energy deposited by other particles.

5. Conclusion

Calibrating the calorimetric mode of underground muon detectors based on plastic scintillators using the average charge from single vertical muons can introduce a bias in the reconstructed muon density. For a detector like the UMD, this reconstruction bias can reach up to 20% for densities of $\sim$30 μ/m^2 in proton showers of $10^{17.5}$ eV. The bias is attributed to the increased energy deposition per muon, especially near shower axis, where higher-energy muons produce more knock-on electrons.

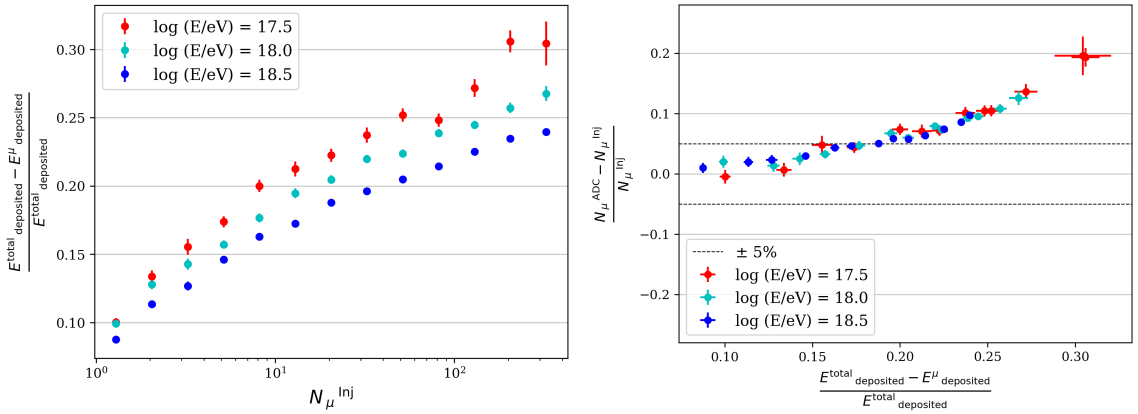

Figure 7: (left) Fraction of energy deposited by particles excluding muons as a function of the number of injected muons per 10 m^2 module. (right) Bias in the muon reconstruction of the ADC mode as a function of the fraction of the energy deposited by particles other than muons.

Within the range where the detector is not saturated, besides muons, knock-on electrons dominate the energy deposition, although protons and other particles like π^+ and K^+ can also contribute slightly. The largest contribution of these particles to the energy deposition was observed for the lowest energy showers of $10^{17.5}$ eV and at the highest muon density of $\sim 30\,\mu/m^2$, where 23% of the total energy is deposited by knock-on electrons and 8% by protons and other particles, mainly π^+ and K^+.

Calibration methods of underground muon detectors based on plastic scintillators should account for variations in the charge with the energy of the incoming muons, or any other related observable. To cope with this issue, a new calibration method in the UMD is presented in Ref. [10].

References

[1] L.G. Dedenko, T.M. Roganova, and G.F. Fedorova, Moscow Univ. Phys. **66** (2011) 358-362.
[2] C. Anderson, G. McKinney, J. Tutt, and M. James, Phys. Proc. **90** (2017) 229-236.
[3] P.H. Stoker, C. Hofmeyr, and C.H. Bornman, Proc. Phys. Soc. **78** (1961) 650.
[4] N. Chaudhuri and M.S. Sinha, Nuovo Cim. **35** (1965) 13-22.
[5] The Pierre Auger Collaboration, JINST **16** (2021) P01026.
[6] S. Agostinelli *et al.*, Nucl. Instrum. Meth. A **506** (2003) 250–303.
[7] S. Argiro *et al.*, Nucl. Instrum. Meth. A **580** (2007) 1485–1496.
[8] The Pierre Auger Collaboration, JINST **16** (2021) P04003.
[9] Particle Data Group *et al.*, Prog. Theor. Exp. Phys. **2020** (2020) P083C01.
[10] The Pierre Auger Collaboration, PoS **UHECR2024** (2024) 077.